

Human umbilical cord mesenchymal stem cells ameliorate erectile dysfunction in rats with diabetes mellitus through the attenuation of ferroptosis

Huan Feng

Tongji Hospital of Tongji Medical College of Huazhong University of Science and Technology

Qi Liu

Shenzhen Baoan Shajing People's Hospital: Shenzhen Baoan Second People's Hospital

Zhiyao Deng

Tongji Hospital of Tongji Medical College of Huazhong University of Science and Technology

Hao Li

Tongji Hospital of Tongji Medical College of Huazhong University of Science and Technology

Huajie Zhang

Shenzhen Baoan Shajing People's Hospital: Shenzhen Baoan Second People's Hospital

Jingyu Song

Tongji Hospital of Tongji Medical College of Huazhong University of Science and Technology

Xiaming Liu

Tongji Hospital of Tongji Medical College of Huazhong University of Science and Technology

Jihong Liu

Tongji Hospital of Tongji Medical College of Huazhong University of Science and Technology

Bo Wen

Shenzhen Baoan Shajing People's Hospital: Shenzhen Baoan Second People's Hospital

Tao Wang (✉ tjhwt@126.com)

Tongji Hospital of Tongji Medical College of Huazhong University of Science and Technology

<https://orcid.org/0000-0003-2952-8397>

Research Article

Keywords: Erectile dysfunction, Human umbilical cord mesenchymal stem cells, Type 1 diabetes mellitus, Type 2 diabetes mellitus, Ferroptosis

Posted Date: April 8th, 2022

DOI: <https://doi.org/10.21203/rs.3.rs-1504898/v1>

License: © ⓘ This work is licensed under a Creative Commons Attribution 4.0 International License.

[Read Full License](#)

Abstract

Background: Erectile dysfunction (ED), as one of the most prevalent consequences in male diabetic patients, has a serious impact on men's physical and mental health, and the treatment effect of diabetic mellitus erectile dysfunction (DMED) is often worse. Therefore, the development of a novel therapeutic approach is urgent. As stem cells with high differentiation potential, human umbilical cord mesenchymal stem cells (HUCMSCs) have been widely used in the treatment of diseases in other systems, and are expected to be a promising strategy for the treatment of DMED. In this study, we investigated the role of HUCMSCs in managing erectile function in rat models of type 1 diabetes mellitus (T1DM) and type 2 diabetes mellitus (T2DM) and compared the effects of two different injection methods.

Methods: T1DM and T2DM ED rats were given labelled HUCMSCs by corpus cavernosum injection and tail vein injection, respectively. ICP and MAP were monitored simultaneously by electrical stimulation four weeks after injection to indicate the erectile function of rats. To track the development and colonisation capabilities of stem cells, we performed EdU assay with penile tissue. The histological changes of the penis were observed by hematoxylin-eosin staining, and Masson's trichrome staining was conducted to evaluate the smooth muscle content and the degree of fibrosis in the rat penis. Then, we employed specific kits to measure the level of NO, cGMP, MDA, SOD and Fe in penis. Electron transmission microscopy was implemented to observe morphology of mitochondria. Besides, western blot and immunofluorescence staining were performed to demonstrate the expression of ferroptosis-related genes.

Results: We found that HUCMSCs improved erectile function in T1DM and T2DM ED rats, with no difference in efficacy between corpus cavernosum injection and tail vein injection. The EdU assay revealed that only a tiny percentage of HUCMSCs colonized the corpus cavernosum, while smooth muscle in the penis expanded and collagen decreased following HUCMSC injection. Moreover, the levels of oxidative stress in the penis of the rats given HUCMSCs were dramatically reduced, as was the tissue iron content. HUCMSCs normalized mitochondrial morphology within corpus cavernosum smooth muscle cells (CCSMCs), which were characteristically altered by high glucose. Furthermore, the expression of ferroptosis inhibitory genes SLC7A11 and GPX4 was obviously elevated in CCSMCs after stem cell management, but the abundances of ACSL4, LPCAT3 and ALOX15 showed the polar opposite tendency.

Conclusions: HUCMSCs can effectively and safely alleviate erectile dysfunction in T1DM and T2DM ED rats, while restoring erectile function by attenuating diabetes-induced ferroptosis in CCSMCs. Additionally, this study provides significant evidence for the development of HUCMSCs as a viable therapeutic strategy for DMED.

Introduction

Erectile Dysfunction (ED) is one of the most common male sexual dysfunction diseases, with 150 million men suffering from varied degrees of ED around the world[1]. As one of the major complications in men with diabetes mellitus (DM), the incidence of ED in diabetic patients is up to 75%[2]. Men with DM tend to

suffer from ED about 10 years earlier than the general population[3]. By 2045, it is estimated that there will be approximately 700 million individuals living with diabetes globally[4]. Despite the fact that PDE5i is now widely acknowledged as a first-line treatment for ED, up to 35% of patients do not react to it[5], which might be owing to diabetes and the consequent severe neurological or vascular lesions. As a result, a more effective therapy for diabetes mellitus erectile dysfunction (DMED) is required.

Mesenchymal stem cells are generated from human bone marrow, umbilical cord tissue, adipose tissue, lung tissue, tooth pulp, and placenta and have immune control, regeneration, and pluripotent differentiation capabilities[6, 7]. Multiple studies have proven that mesenchymal stem cells may be utilised to treat corticosteroid-resistant graft-versus-host disease, multiple sclerosis, osteoarthritis, heart failure, and other indications without substantial adverse effects[8–11].

Human umbilical cord mesenchymal stem cells (HUCMSCs) have a number of benefits over stem cells generated from other organs. To begin with, the collection of HUCMSCs is non-invasive, which reduces the risk of infection significantly. HUCMSCs, on the other hand, have a greater proliferation capacity and can sustain steady growth after the tenth passage, suggesting that they might theoretically have better therapeutic effectiveness at the same dosage[12]. Second, due to their distinct gene expression profile, HUCMSCs are barely tumorigenic and have a higher differentiation capability and self-renewal potential[12]. Low expression of major histocompatibility complex (MHC) class I molecules, a significant absence of MHC class II molecules, and a lack of co-stimulatory ligands such as CD40, CD80, and CD86 further reduced the immunogenicity of HUCMSCs[15]. As a result, it's clear that HUCMSCs might be an excellent therapy option.

Some clinical trials have indicated that HUCMSCs can safely and effectively treat lung damage and improve decreased lung function in patients with COVID-19 in recent years[16, 17]. HUCMSCs also improved in-situ healing capabilities in rhesus monkeys with severe uterine adhesions and decreased mortality in rats with ARDS accompanied by sepsis, according to two other preclinical investigations[18, 19]. Based on these findings, we created animal models of T1DM and T2DM ED rats, with the goal of determining the possible therapeutic benefits of HUCMSCs on DMED and investigating the underlying processes.

Materials And Methods

1. Cell identification and culture

HUCMSCs were donated by Shandong Qilu Cell Therapy Technology Co., Ltd and suspended in specialised medium (Dulbecco's modified Eagle's medium [DMEM, Gibco, USA] with supplements for HUCMSCs [Qilu Cell Therapy Technology, China]) and cultivated at 37°C in a 5% CO₂ incubator. The fourth passage HUCMSCs were identified by flow cytometry. Flow cytometry was used to identify the HUCMSCs in the fourth passage. For surface marker verification, the following antibodies were used: CD29, CD31, CD34, CD45, CD90, and CD105 (BD Biosciences, USA).

The multilineage differentiation potential of HUCMSCs was examined using third passage cells, as previously described. For 14 days, cells were grown in adipogenic medium (DMEM containing 10% FBS, 2 mM dexamethasone, 2 mg/L insulin, 0.5 mM 3-isobutyl-1-methylxanthine, 0.2 mM indomethacin) and for 28 days in osteogenic medium (DMEM containing 10% FBS, 2 mM dexamethasone, 1 M sodium glycerol phosphate, 10 mM vitamin C). The capacity to develop into adipocytes and osteoblasts was then assessed using Oil red O and Alizarin red S staining.

Our team's typical approach involved isolating corpus cavernosum smooth muscle cells (CCSMCs) from rat penis and purifying them using a differential adhesion method over the course of two weeks[20]. The CCSMCs were then grown in DMEM with 10% FBS added. CCSMCs were detected by immunofluorescence using antibodies against α -smooth muscle actin (α -SMA; 1:200; Affinity Biosciences, AF1032, USA) and desmin (1:200; Affinity Biosciences, AF5334, USA).

The co-culture system was constructed by a polycarbonate membrane of Costar Transwell Inserts (Corning, No.3412, USA). The upper and lower chambers were seeded with CCSMCs and HUCMSCs, respectively.

2. Experiments with animals

Thirty 7-week-old male Sprague-Dawley (SD) rats and thirty 7-week-old male Zucker Diabetic Fatty (ZDF) rats were obtained from Beijing Vital River Laboratory Animal Technology Co., Ltd., and they were all fed adaptively for 7 days after fasting overnight. For type 1 diabetes mellitus (T1DM), streptozotocin (STZ; 60 mg/kg; Sigma-Aldrich) was diluted in citrate phosphate buffer (50mM; pH = 4.5) and injected intraperitoneally into SD rats. The rest 6 SD rats were administrated with the same buffer and placed in the control group. The blood glucose levels of all SD rats were measured three and seven days later, and rats with fasting blood glucose > 16.7 mmol/L at both tests were classified as T1DM. Purina5008 was given to ZDF rats for 4 weeks to induce type 2 diabetic mellitus (T2DM). The remaining seven rats were designated as the control group and continued to be fed with standard chow. The blood glucose levels of ZDF rats were tested three- and seven-days following induction feeding, and animals with fasting blood glucose levels > 16.7 mmol/L at both assessments were defined as T2DM.

Ten weeks later, all of DM rats survived. Following that, an apomorphine (APO) test was performed to identify the rats with DM ED, and those with a negative erection were classified as DMED rats, as in the prior study[21]. Through the APO test, 18 rats each were diagnosed with T1DM and T2DM ED. SD rats were further separated into four groups (DMED group, n = 5; DMED + corpus cavernosum injection (CI) group, n = 7; DMED + tail vein injection (VI) group, n = 6; control group, n = 6). Meanwhile, ZDF rats were separated into four groups (DMED group, n = 5; DMED + corpus cavernosum injection (CI) group, n = 7; DMED + tail vein injection (VI) group, n = 6; control group, n = 7). Two of the groups (the DMED + CI group and DMED + VI group) received HUCMSCs injections at different sites, whereas the DMED group and the control group received saline treatment. Moreover, HUCMSCs were labelled with 5-ethynyl-2'-deoxyuridine (EdU; Beyotime, China).

3. Erectile function evaluation

The intracavernous pressure (ICP) was monitored four weeks following injection, as previously described[21]. Ketamine (100 mg/kg) and midazolam (5 mg/kg) were used to anaesthetize rats. To measure ICP, a 25-gauge needle was placed into the left penile crus. With micro scissors, a V-shaped incision was created in the carotid artery, a PE-50 tube was inserted, and it was ligated and fastened. The PE tube was pre-filled with heparinized saline (200 IU/mL) and attached to a signal collection device (AD Instruments, Australia), allowing for continuous monitoring of mean arterial pressure (MAP). After that, bipolar electrodes were used to electrically activate the cavernous nerve (15.0 Hz; 5.0 V; for 1 minutes). The ratio of maximum ICP (max ICP) to MAP (max ICP/MAP) was used to determine erectile function. The rats were slaughtered after their erectile function was assessed, and the penises were dissected from the original tissue. For histologic research, one third of the penis was preserved in paraffin, while the rest were kept at 80°C for other experiments.

4. Immunohistochemistry, hematoxylin-eosin (H&E) staining, and Masson's trichrome staining

Immunohistochemistry was performed as previously reported[23]. After antigen retrieval and dewaxed, sections of corpus cavernosum were incubated with antibodies against endothelial nitric oxide synthase (eNOS; 1:100; Affinity Biosciences, AF0096, USA) or neuronal nitric oxide synthase (nNOS; 1:100; Affinity Biosciences, AF6249, USA) antibodies, followed by biotinylated secondary antibodies.

The tissues were fixed for 24 hours in 4% paraformaldehyde (Servicebio, China) before being imbedded in paraffin. Serial 4 µm paraffin-embedded slices were obtained and dewaxed in xylene I and xylene II for 10 minutes each, before being rehydrated in a variety of ethanol concentrations (100% for 5 min, 100% for 5 min, 95% 5 minutes, 90% 5 minutes, 80% 5 minutes, 70% 5 minutes). The slices were then washed three times in distilled water (5 minutes each). Finally, according to the manufacturer's instructions, sections were stained with H&E solution (Servicebio, China).

Masson's trichrome staining was conducted according to the standard protocol. The ratio of smooth muscle to collagen was taken as an indicator of the degree of fibrosis in the corpus cavernosum.

5. Fluorescence staining

A superoxide anion fluorescent probe (Dihydroethidium, DHE; Yeasen Biotechnology) and the Reactive Oxygen Species Assay Kit (2,7-Dichlorodi-hydrofluorescein diacetate, DCFH-DA; Yeasen Biotechnology) were used to measure the quantity of reactive oxygen species (ROS) in the corpus cavernosum. DHE and DCFH-DA were used to incubate tissue and cell sections, respectively.

As previously stated, penis samples were preprocessed. GPX4 (1:200; ABclonal, A1933, China) and ACSL4 (1:200; ABclonal, A1933, China) were used to incubate sections (1:200; Affinity Biosciences, DF12141, USA). The slides were then treated with the appropriate secondary antibodies before being stained with 4', 6-diamidino-2-phenylindole (DAPI, Invitrogen) for nuclear staining.

Sections were assessed for EdU labelling using the BeyoClick™ EdU Assay Kit with Alexa Fluor 647 (Beyotime, China), for 30 minutes at room temperature. The above sections were inspected under a fluorescence microscope.

6. Measurement of oxidative activity

The levels of malondialdehyde (MDA) and superoxide dismutase (SOD) reflected the oxidative and antioxidant activities, respectively. The Micro MDA Assay Kit (Solarbio, BC0025, China) and SOD assay kit (Nanjing Jiancheng Bioengineering Institute, A001-3-2, China) were used to detect these two indicators according to the manufacturer's instructions.

7. Assessment of iron content

The content of Fe in corpus cavernosum was evaluated by Tissue Iron Assay Kit (Nanjing Jiancheng Bioengineering Institute, A039-2-1, China) according to the manufacturer's instructions.

8. Examination of nitric oxide (NO) and cyclic guanosine monophosphate (cGMP) levels

Nitrate-nitrite Assay Kit (Beyotime, S0024, China) was used to detect the level of NO, and the cGMP levels were determined ELISA kit (R&D Systems, F15182, USA) according to the standard protocol. The results were normalised to the protein concentration.

9. Transmission electron microscope (TEM) analysis

Cells were fixed with Electron Microscope Fixative Solution (Servicebio, G1102, China) for 1 hour, then were re-fixed with 1% osmic acid in 0.1 M phosphate buffered saline (pH 7.4) at room temperature for 2 hours. Next, adding 50%, 70%, 80%, 90%, 95%, 100% and 100% ethanol to dehydrate in sequence, 15min each time. Finally, they were embedded in SPI-Pon 812 (SPI, 0529-77-4, USA). An ultramicrotome (UC, Leica) was used to cut 60nm ultrathin sections, which were stained with 2% uranyl acetate and lead citrate, subsequently. Sections were examined under a Hitachi electron microscope (Hitachi, HT7800, Japan).

10. Western blotting

Proteins were extracted by RIPA lysis buffer (Boster, AR0102, China) supplemented with 1% PMSF (Boster, AR1178, China), 1% protease inhibitor (Boster, AR1182, China) and 1% protease inhibitor cocktail (MCE, HY-K0010, China). SDS-PAGE was used to separate the proteins, which were then transferred to PVDF membranes. After blocking with Tris-buffered saline-Tween with 5% bovine serum albumin for 1 hour at room temperature, membranes were incubated with primary antibodies against SLC7A11 (1:500; ABclonal, A13685, China), GPX4 (1:500; ABclonal, A1933, China), ACSL4(1:1000; Affinity Biosciences, DF12141, USA), LPCAT3 (1:500; ABclonal, A17604, China), ALOX15 (1:500; ABclonal, A6864, China) and β -Actin (1:200000; ABclonal, AC026, China) at 4°C overnight. Then, the membranes were hybridized with

goat anti-rabbit secondary antibody (1:10000; Boster, BA1055, China) and visualized by ChemiDoc Touch Imaging System (Bio-Rad, USA).

11. Reagent

RSL3 is one of ferroptosis agonists. CCSMCs were exposed to 500 nmol/L RSL3 (MCE, HY-100218A, China) for 24 hours in order to induce ferroptosis. Ferroptosis inhibitor ferrostatin-1 (Fer-1; 1 μ mol/L; MCE, HY-100579, China) was added to medium to inhibit ferroptosis in CCSMCs.

12. Statistical analysis

The photos were examined by Image-Pro Plus 6.0 software, and results were analysed with GraphPad Prism 8.3. Statistical analyses were conducted using one-way ANOVA followed by the Tukey's test for *post hoc* comparisons. $P < 0.05$ was defined as statistically significant.

Results

1. Characterization of HUCMSCs and CCSMCs

The isolated stem cells showed typical fibroblast morphology when they were passed to the third passage (**Figure. 1A**). To identify HUCMSCs, we used flow cytometry to detect the expression of specific markers. As shown in the **Figure. 1B**, most cells expressed CD29, CD90, and CD105, although CD31, CD34, and CD45 were seldom expressed. Meanwhile, with the multipotency of HUCMSCs, we successfully induced them into adipocytes and osteoblasts, which indicated by Oil red O staining and Alizarin red S staining, respectively (**Figure. 1C, D**).

CCSMCs were isolated from rat penis, as in our prior investigation[20]. The cells were then identified by immunofluorescence staining (**Figure. 1E**), which revealed that they exhibited significant levels of α -SMA and desmin, suggesting that the cells we extracted and cultivated were CCSMCs.

2. Metabolic indices

As illustrated in **Figure. 2**, there was no significant difference in the initial body weight and fasting blood glucose among all groups, whether T1DM or T2DM rats. In T1DM rats, the DMED group, CI group, and VI group had higher blood glucose and lower body weight than the control group ten weeks after induction, but in T2DM rats, the DMED group, CI group, and VI group had higher blood glucose and body weight than the control group. These findings consistently demonstrated that we had successfully created a rat model of T1DM and T2DM.

3. HUCMSCs could improve erectile function in DMED rats

The ratio of max ICP to MAP reflected erectile function. In T1DM rats (**Figure. 3A, 3C**), the indicator was dramatically reduced in the DMED group and significantly improved following injection of HUCMSCs into

the corpus cavernosum or tail vein. It also revealed a consistent trend in T2DM rats at the same period (**Figure. 3B, D**).

4. HUCMSCs suppressed penile histological changes *in vivo*

We detected the colonisation of stem cells by EdU assay (**Figure. S1**), however only very low fluorescence intensity was seen in the penile tissue of type 1 and type 2 DMED rats following stem cell injection. The corpus cavernosum smooth muscle atrophy was discovered in the diabetic group (**Figure. 4B**). The smooth muscle regeneration and reduction in cavernous fibrosis, on the other hand, occurred in the CI and VI groups, and the smooth muscle/collagen ratio rose considerably in both groups (**Figure. 4C, D**). Importantly, following HUCMSC injection, there was no substantial alteration in the anatomy of the rat penis, no inflammation, no tissue necrosis, and no tumour growth in the corpus cavernosum (**Figure. 4A**).

5. HUCMSCs retained NO activity *in vivo*

We employed particular kits to quantify NO and cGMP concentrations in rat penises, same as we did in our previous work[24]. NO and cGMP production in the penis of DMED rats were severely suppressed, although they were somewhat enhanced after stem cell injection, according to the findings (**Figure. S2A-D**). We next used immunohistochemistry to examine the quantity of eNOS and nNOS in the rat penis, two enzymes that mediated the synthesis of NO in the corpus cavernosum for erection maintenance. The levels of eNOS and nNOS in the DMED group were found to be lower than those in the control group, whereas they were somewhat higher in the CI and VI groups (**Figure. S2E, F**).

6. HUCMSCs reduced iron content and inhibited oxidative stress *in vivo*

To explore and confirm the role of ferroptosis in DMED, we examined the iron content and oxidative stress in rat penis. The results revealed that the iron content in DMED rats' penis was much higher, but the iron content of rats in the CI and VI groups was significantly lower, which was observed in both T1DM and T2DM rats (**Figure. 5A, B**). MDA levels exhibited a similar trend as a sign of oxidative stress, and HUCMSCs obviously reduced MDA concentration in DMED rats (**Figure. 5C, D**). In contrast, SOD acted as an antioxidant in the body and exhibited the exact opposite changes to MDA (**Figure. 5E, F**). Then, DHE staining was conducted in the corpus cavernosum to reflect ROS (**Figure. 6**). The results showed that ROS expression was higher in the DMED group, and HUCMSCs attenuated ROS production significantly in the CI and VI groups.

7. HUCMSCs decreased oxidative stress *in vitro*

In order to confirm the inhibitory effect of HUCMSCs on oxidative stress *in vitro*. We cultivated HUCMSCs and CCSMCs in the co-culture system (**Figure. 7A**). The amount of ROS was measured by DCFH-DA staining (**Figure. 7B, C**). The findings demonstrated that smooth muscle cells produced more ROS than usual in a high-glucose environment and after RSL3 treatment, and that the quantity of ROS dropped dramatically after co-culture with HUCMSCs, but CCSMCs exposed to the ferroptosis inhibitor Fer-1 showed a consistent trend.

8. HUCMSCs attenuated ferroptosis through SLC7A11/GPX4/ACSL4 pathway *in vitro*

Mitochondria in ferroptotic cells exhibited specific morphological changes. We observed the shrunken mitochondria, decreased or complete absence of mitochondria cristae and high electron density in RSL3-treated CCSMCs by electron microscopy. Meanwhile, CCSMCs treated with high glucose displayed comparable alterations, suggesting that diabetes might cause ferroptosis in CCSMCs. However, after co-culturing with HUCMSCs, the morphological changes in mitochondria were significantly improved, and normal mitochondrial structure could be observed (**Figure. 7D**).

As an important component of the cystine transporter system Xc^- , SLC7A11-mediated cystine uptake plays a vital role in inhibiting cellular oxidative stress. In Fig. 8, the expression of SLC7A11 in CCSMCs treated with high glucose and RSL3 was significantly lower than in normal cells, according to Western blot analysis, and HUCMSCs had a clear ability to rescue its expression, which was consistent with CCSMCs treated with Fer-1. GPX4 is one of the most well-known ferroptosis defence pathways, and its expression in each group followed the same pattern as SLC7A11. While ACSL4, LPCAT3, and ALOX15, which promote oxidative stress during ferroptosis, were clearly elevated in CCSMCs treated with high glucose, they were significantly reduced after co-culture with HUCMSCs.

Discussion

It's been reported that the global incidence of erectile dysfunction is expected to rise to 322 million cases by 2025[1, 25, 26]. Diabetes is a major risk factor for erectile dysfunction, and peripheral neuropathy, atherosclerosis of large vessels, endothelial dysfunction of small arteries and hypogonadism can eventually lead to erectile dysfunction[27–30]. We investigated the effect of HUCMSCs on DMED rats' erectile function through corpus cavernosum injection and tail vein injection, respectively, based on the construction of T1DM and T2DM ED rats. The impaired erectile function of DMED rats was significantly improved without side effects, and the underlying molecular mechanism by which HUCMSCs could attenuate ferroptosis in CCSMCs was confirmed, all of which indicated that HUCMSCs could be a promising emerging therapeutic strategy for DMED.

HUCMSCs, a kind of naïve stem cell found in the human body, may be collected in great quantities without posing a risk to the donor, and the application of HUCMSCs does not raise ethical problems. In recent years, some studies have revealed that bone mesenchymal stem cells (BMSCs) and adipose-derived stem cells (ADSCs) could improve the erectile function of DMED to some extent[31, 32], similar to how HUCMSCs have been shown to have good therapeutic effects on diseases of the immune system, cardiovascular system, and digestive system[33–35]. The real therapeutic benefits of BMSCs and ADSCs to DMED, however, are restricted due to their high degree of differentiation and low biological stability[36–40]. Furthermore, certain clinical trials have showed that PDE5i is still necessary to sustain erection following the administration of BMSCs or ADSCs[41, 42]. T1DM and T2DM rats given HUCMSCs had considerable improvement in their erectile function, and there were no evident rejection or other adverse effects following injection, demonstrating the biological safety of HUCMSCs. The favourable

impact of stem cells in tissue repair, according to Matz et al., is more dependent on paracrine activity, the production of cytokines and growth factors that reduce inflammation and promote healing, than on colonisation and differentiation[43]. We labelled the cells with EdU before injecting them to investigate the exact mechanism of HUCMSCs in the treatment of DMED[44–46]. It revealed that only a small number of labelled HUCMSCs colonised the rat penis, implying that HUCMSCs primarily repair tissue via paracrine. Päch et al. also disclosed that, despite not having successfully differentiated into β cells, mesenchymal stem cells (MSCs) can secrete a variety of immunomodulatory and tissue regeneration factors to lower blood glucose levels[47]. In several clinical trials, researchers discovered that MSCs reduced and delayed the destruction of β cells in many T1DM patients, but did not restore their function[48–50]. And the anti-inflammatory properties of MSCs were exploited to treat chronic low-grade inflammation in T2DM patients, which was thought to be a major cause of insulin resistance and β -cell dysfunction[51]. Interestingly, we noticed that there was a slight improvement in hyperglycemia in T2DM ED rats after injection, but not in T1DM ED rats, even though HUCMSCs did not restore fasting glucose to normal in both types of DMED rats. Based on these, we preliminarily confirmed that HUCMSCs ameliorated ED through a glucose independent manner. On the other hand, more severe hyperglycemia might exacerbate irreversible damage to pancreatic cells, vascular smooth muscle cells, vascular endothelial cells, and cavernous nerves in T1DM rats.

Stem cell treatment for ED was previously administered mostly through the corpus cavernosum, abdominal cavity, and tail vein. There was only one study comparing the efficacy of corpus cavernosum and tail vein injection of ADSCs in rats with nerve-injured ED[52]. In fact, DMED is currently more common than nerve-injured ED. Our findings are the first to compare the therapeutic effects of HUCMSCs on two types of DMED rats by CI and VI. The therapeutic effects of the two methods are almost identical, and there are no obvious differences in various indicators. It was demonstrated that HUCMSCs could effectively improve the erectile function of rats through CI and VI. This could serve as a starting point for future research on HUCMSCs as a DMED treatment.

As revealed by Masson's trichrome staining, we found that the ability of HUCMSCs to suppress cavernous fibrosis might contribute to their therapeutic impact in ED. One of the key causes of DMED, as revealed in a previous study[53, 54], is corpus cavernosum fibrosis, which is induced by reduced corpus cavernosum smooth muscle and increased collagen. In both types of DMED rats, we noticed a considerable loss in smooth muscle and a significant rise in collagen, but these histological alterations were greatly relieved following stem cell therapy, indicating that HUCMSCs had a good anti-fibrotic activity.

NO causes the corpus cavernosum smooth muscle to relax by promoting the synthesis of cGMP in CCSMCs, which is produced by eNOS in cavernous endothelial cells and nNOS in cavernous neurons. Our data argued that HUCMSCs might increase the abundance of eNOS and nNOS in the corpus cavernosum of DMED rats, boosting NO and cGMP levels, implying that HUCMSCs could alleviate DMED via the NO/cGMP pathway.

Ferroptosis plays a crucial role in the occurrence and progression of various diseases, and regulating the ferroptosis pathway presents a potential therapeutic strategy for many diseases[55–57]. The intracellular antioxidant system, System Xc⁻, is made up of two subunits, SLC7A11 and SLC3A2. Through the System Xc⁻, cysteine and glutamic acid collaborate to synthesise glutathione, and glutathione then lowers ROS and reactive nitrogen via glutathione peroxidase (GPX). Inhibition of System Xc⁻ function interferes with GSH production, resulting in reduced GPX activity, decreased cellular antioxidant capacity, lipid ROS buildup, and, ultimately, oxidative damage and ferroptosis[58]. GPX4, member of the GPX family, is a critical regulator of ferroptosis via limiting the formation of lipid peroxides. GPX4 converts glutathione to oxidised glutathione peptide (GSSG), and reduce cytotoxic lipid peroxidation to the corresponding alcohol. Inhibition of GPX4 activity leads to accumulation of lipid peroxides, a hallmark of ferroptosis[59]. However, the role of ferroptosis in ED remains unclear. First, we found that HUCMSCs diminished iron content and oxidative stress levels in DMED rats' penis, including MDA, SOD, and ROS. Second, HUCMSCs were able to enhance the abundance of SLC7A11 and GPX4 while decreasing the expression of lipid metabolism-related genes such ACSL4, LPCAT3, and ALOX15. Furthermore, intracellular mitochondria treated with high glucose showed morphological abnormalities that were rescued by HUCMSCs. Those proved that HUCMSCs might alleviate DMED by prohibiting the ferroptosis signalling pathway in CCSMCs.

There are some limitations in current study. We utilized the DMED rat model to explore the impact of HUCMSCs on DMED and the underlying mechanism, however additional study is needed to better understand its safety, effectiveness, and other unknown concerns before it can be used in clinical practise. In the following investigation, we'll build rabbit, dog, and possibly monkey animal models to further confirm the therapeutic efficacy of HUCMSCs on DMED. Second, the injection dose used in the study was one million cells, which is consistent with other studies[60–64]. It is unclear whether there is an ideal dose yet, therefore we will compare outcomes from different doses in future studies to find the optimal injection dose.

Conclusions

In summary, the current investigation found that HUCMSCs improved erectile function in T1DM and T2DM ED rats without major adverse events. Moreover, it was uncovered that HUCMSCs not only inhibited corpus cavernosum fibrosis and activated NOS, but prevented diabetes-induced ferroptosis in CCSMCs. Furthermore, we found that HUCMSCs possessed equal efficacy in the therapy of DMED when injected into the corpus cavernosum and tail vein. These findings provide preclinical evidence for a potential treatment for DMED and new insights into the therapeutic mechanism of HUCMSCs in the treatment of DMED.

Abbreviations

ED: erectile dysfunction; DMED: diabetic mellitus erectile dysfunction; HUCMSCs: human umbilical cord mesenchymal stem cells; T1DM: type 1 diabetes mellitus; T2DM: type 2 diabetes mellitus; CCSMCs:

corpus cavernosum smooth muscle cells; DM: diabetes mellitus; MHC: major histocompatibility complex; DMED: Dulbecco's modified Eagle's medium; SD: Sprague-Dawley; ZDF: Zucker Diabetic Fatty; APO: apomorphine; CI: corpus cavernosum injection; VI: tail vein injection; EdU: 5-ethynyl-2'-deoxyuridine; ICP: intracavernous pressure; MAP: mean arterial pressure; H&E: hematoxylin-eosin; eNOS: endothelial nitric oxide synthase; nNOS: neuronal nitric oxide synthase; DAPI: 4', 6-diamidino-2-phenylindole; MDA: malondialdehyde; SOD: superoxide dismutase; cGMP: cyclic guanosine monophosphate; NO: nitric oxide; TEM: transmission electron microscope; BMSCs: bone mesenchymal stem cells; ADSCs: adipose-derived stem cells; MSCs: mesenchymal stem cells; GPX: glutathione peroxidase; GSSG: glutathione peptide

Declarations

Ethics approval and consent to participate

The animal study was reviewed and approved by Experimental Animal Administration Committee of Wuhan Servicebio Biotechnology.

Acknowledgements

We would like to thank Shandong Qilu Cell Therapy Technology Co., Ltd for its help.

Authors' contributions

WT and HF contributed to the conception. HF, ZD, HL and JS performed the whole experimental work. HF, QL and HZ contributed to data acquisition and analysis. HF and XL drafted the work. TW, BW, and JL supervised the work. All authors read and approved the final manuscript.

Funding

This work was supported by the Natural Science Foundation of Shenzhen [JCYJ20210324134400002 & JCYJ20210324141404010] and Hubei Provincial Medical Youth Top Talent Project.

Availability of data and materials

The data that support the findings of this study are available from the corresponding author upon reasonable request.

Consent for publication

Not applicable.

Competing interests

The authors have declared that no competing interest exists.

References

1. Burnett AL, Nehra A, Breau RH, Culkin DJ, Faraday MM, Hakim LS, et al. Erectile Dysfunction: AUA Guideline. *J Urol*. 2018;200:633–41.
2. Kouidrat Y, Pizzol D, Cosco T, Thompson T, Carnaghi M, Bertoldo A, et al. High prevalence of erectile dysfunction in diabetes: a systematic review and meta-analysis of 145 studies. *Diabet Med*. 2017;34:1185–92.
3. Johannes CB, Araujo AB, Feldman HA, Derby CA, Kleinman KP, McKinlay JB. Incidence of erectile dysfunction in men 40 to 69 years old: longitudinal results from the Massachusetts male aging study. *J Urol*. 2000;163:460–3.
4. Tonnie T, Rathmann W, Hoyer A, Brinks R, Kuss O. Quantifying the underestimation of projected global diabetes prevalence by the International Diabetes Federation (IDF) Diabetes Atlas. *BMJ Open Diabetes Res Care*. 2021;9.
5. Shamloul R, Ghanem H. Erectile dysfunction. *Lancet*. 2013;381:153–65.
6. Galipeau J, Sensebe L. Mesenchymal Stromal Cells: Clinical Challenges and Therapeutic Opportunities. *Cell Stem Cell*. 2018;22:824–33.
7. Behnke J, Kremer S, Shahzad T, Chao CM, Bottcher-Friebertshauser E, Morty RE, et al. MSC Based Therapies-New Perspectives for the Injured Lung. *J Clin Med*. 2020;9.
8. Ball LM, Bernardo ME, Roelofs H, van Tol MJ, Contoli B, Zwaginga JJ, et al. Multiple infusions of mesenchymal stromal cells induce sustained remission in children with steroid-refractory, grade III-IV acute graft-versus-host disease. *Br J Haematol*. 2013;163:501–9.
9. Muraro PA, Martin R, Mancardi GL, Nicholas R, Sormani MP, Saccardi R. Autologous haematopoietic stem cell transplantation for treatment of multiple sclerosis. *Nat Rev Neurol*. 2017;13:391–405.
10. Pas HI, Winters M, Haisma HJ, Koenis MJ, Tol JL, Moen MH. Stem cell injections in knee osteoarthritis: a systematic review of the literature. *Br J Sports Med*. 2017;51:1125–33.
11. Guo R, Morimatsu M, Feng T, Lan F, Chang D, Wan F, et al. Stem cell-derived cell sheet transplantation for heart tissue repair in myocardial infarction. *Stem Cell Res Ther*. 2020;11:19.
12. Lu LL, Liu YJ, Yang SG, Zhao QJ, Wang X, Gong W, et al. Isolation and characterization of human umbilical cord mesenchymal stem cells with hematopoiesis-supportive function and other potentials. *Haematologica*. 2006;91:1017–26.
13. Fong CY, Chak LL, Biswas A, Tan JH, Gauthaman K, Chan WK, et al. Human Wharton's jelly stem cells have unique transcriptome profiles compared to human embryonic stem cells and other mesenchymal stem cells. *Stem Cell Rev Rep*. 2011;7:1–16.
14. Hsieh JY, Fu YS, Chang SJ, Tsuang YH, Wang HW. Functional module analysis reveals differential osteogenic and stemness potentials in human mesenchymal stem cells from bone marrow and Wharton's jelly of umbilical cord. *Stem Cells Dev*. 2010;19:1895–910.
15. Cho PS, Messina DJ, Hirsh EL, Chi N, Goldman SN, Lo DP, et al. Immunogenicity of umbilical cord tissue derived cells. *Blood*. 2008;111:430–8.

16. Meng F, Xu R, Wang S, Xu Z, Zhang C, Li Y, et al. Human umbilical cord-derived mesenchymal stem cell therapy in patients with COVID-19: a phase 1 clinical trial. *Signal Transduct Target Ther.* 2020;5:172.
17. Shi L, Huang H, Lu X, Yan X, Jiang X, Xu R, et al. Effect of human umbilical cord-derived mesenchymal stem cells on lung damage in severe COVID-19 patients: a randomized, double-blind, placebo-controlled phase 2 trial. *Signal Transduct Target Ther.* 2021;6:58.
18. Wang L, Yu C, Chang T, Zhang M, Song S, Xiong C, et al. In situ repair abilities of human umbilical cord-derived mesenchymal stem cells and autocrosslinked hyaluronic acid gel complex in rhesus monkeys with intrauterine adhesion. *Sci Adv.* 2020;6:a6357.
19. Lee FY, Chen KH, Wallace CG, Sung PH, Sheu JJ, Chung SY, et al. Xenogeneic human umbilical cord-derived mesenchymal stem cells reduce mortality in rats with acute respiratory distress syndrome complicated by sepsis. *Oncotarget.* 2017;8:45626–42.
20. Zhang Y, Yang J, Zhuan L, Zang G, Wang T, Liu J. Transplantation of adipose-derived stem cells overexpressing inducible nitric oxide synthase ameliorates diabetes mellitus-induced erectile dysfunction in rats. *Peerj.* 2019;7:e7507.
21. Song J, Tang Z, Li H, Jiang H, Sun T, Lan R, et al. Role of JAK2 in the Pathogenesis of Diabetic Erectile Dysfunction and an Intervention With Berberine. *J Sex Med.* 2019;16:1708–20.
22. Yuan P, Ma D, Gao X, Wang J, Li R, Liu Z, et al. Liraglutide Ameliorates Erectile Dysfunction via Regulating Oxidative Stress, the RhoA/ROCK Pathway and Autophagy in Diabetes Mellitus. *Front Pharmacol.* 2020;11:1257.
23. Song J, Sun T, Tang Z, Ruan Y, Liu K, Rao K, et al. Exosomes derived from smooth muscle cells ameliorate diabetes-induced erectile dysfunction by inhibiting fibrosis and modulating the NO/cGMP pathway. *J Cell Mol Med.* 2020;24:13289–302.
24. Luan Y, Cui K, Tang Z, Ruan Y, Liu K, Wang T, et al. Human Tissue Kallikrein 1 Improves Erectile Dysfunction of Streptozotocin-Induced Diabetic Rats by Inhibition of Excessive Oxidative Stress and Activation of the PI3K/AKT/eNOS Pathway. *Oxid Med Cell Longev.* 2020;2020:6834236.
25. Bacon CG, Mittleman MA, Kawachi I, Giovannucci E, Glasser DB, Rimm EB. Sexual function in men older than 50 years of age: results from the health professionals follow-up study. *Ann Intern Med.* 2003;139:161–8.
26. Ayta IA, McKinlay JB, Krane RJ. The likely worldwide increase in erectile dysfunction between 1995 and 2025 and some possible policy consequences. *Bju Int.* 1999;84:50–6.
27. Yafi FA, Jenkins L, Albersen M, Corona G, Isidori AM, Goldfarb S, et al. Erectile dysfunction. *Nat Rev Dis Primers.* 2016;2:16003.
28. Corona G, Giorda CB, Cucinotta D, Guida P, Nada E. The SUBITO-DE study: sexual dysfunction in newly diagnosed type 2 diabetes male patients. *J Endocrinol Invest.* 2013;36:864–8.
29. Corona G, Giorda CB, Cucinotta D, Guida P, Nada E. Sexual dysfunction at the onset of type 2 diabetes: the interplay of depression, hormonal and cardiovascular factors. *J Sex Med.* 2014;11:2065–73.

30. Corona G, Rastrelli G, Balercia G, Lotti F, Sforza A, Monami M, et al. Hormonal association and sexual dysfunction in patients with impaired fasting glucose: a cross-sectional and longitudinal study. *J Sex Med.* 2012;9:1669–80.
31. Lu J, Xin Z, Zhang Q, Cui D, Xiao Y, Zhuo J, et al. Beneficial effect of PEDF-transfected ADSCs on erectile dysfunction in a streptozotocin-diabetic rat model. *Cell Tissue Res.* 2016;366:623–37.
32. Qiu X, Lin H, Wang Y, Yu W, Chen Y, Wang R, et al. Intracavernous transplantation of bone marrow-derived mesenchymal stem cells restores erectile function of streptozocin-induced diabetic rats. *J Sex Med.* 2011;8:427–36.
33. He X, Yang Y, Yao M, Yang L, Ao L, Hu X, et al. Combination of human umbilical cord mesenchymal stem (stromal) cell transplantation with IFN-gamma treatment synergistically improves the clinical outcomes of patients with rheumatoid arthritis. *Ann Rheum Dis.* 2020;79:1298–304.
34. Kim HS, Shin TH, Lee BC, Yu KR, Seo Y, Lee S, et al. Human umbilical cord blood mesenchymal stem cells reduce colitis in mice by activating NOD2 signaling to COX2. *Gastroenterology.* 2013;145:1392–403.
35. Bartolucci J, Verdugo FJ, Gonzalez PL, Larrea RE, Abarzua E, Goset C, et al. Safety and Efficacy of the Intravenous Infusion of Umbilical Cord Mesenchymal Stem Cells in Patients With Heart Failure: A Phase 1/2 Randomized Controlled Trial (RIMECARD Trial [Randomized Clinical Trial of Intravenous Infusion Umbilical Cord Mesenchymal Stem Cells on Cardiopathy]). *Circ Res.* 2017;121:1192–204.
36. Liu G, Sun X, Bian J, Wu R, Guan X, Ouyang B, et al. Correction of diabetic erectile dysfunction with adipose derived stem cells modified with the vascular endothelial growth factor gene in a rodent diabetic model. *PLoS ONE.* 2013;8:e72790.
37. Jeon SH, Zhu GQ, Bae WJ, Choi SW, Jeong HC, Cho HJ, et al. Engineered Mesenchymal Stem Cells Expressing Stromal Cell-derived Factor-1 Improve Erectile Dysfunction in Streptozotocin-Induced Diabetic Rats. *Int J Mol Sci.* 2018;19.
38. Das ND, Song KM, Yin GN, Batbold D, Kwon MH, Kwon KD, et al. Xenogenic transplantation of human breast adipose-derived stromal vascular fraction enhances recovery of erectile function in diabetic mice. *Biol Reprod.* 2014;90:66.
39. Wang X, Liu C, Xu Y, Chen P, Shen Y, Xu Y, et al. Combination of mesenchymal stem cell injection with icariin for the treatment of diabetes-associated erectile dysfunction. *PLoS ONE.* 2017;12:e174145.
40. Yang Q, Chen W, Zhang C, Xie Y, Gao Y, Deng C, et al. Combined Transplantation of Adipose Tissue-Derived Stem Cells and Endothelial Progenitor Cells Improve Diabetic Erectile Dysfunction in a Rat Model. *Stem Cells Int.* 2020;2020:2154053.
41. Yiou R, Hamidou L, Birebent B, Bitari D, Lecorvoisier P, Contremoulins I, et al. Safety of Intracavernous Bone Marrow-Mononuclear Cells for Postradical Prostatectomy Erectile Dysfunction: An Open Dose-Escalation Pilot Study. *Eur Urol.* 2016;69:988–91.
42. Matz EL, Terlecki RP. Stem Cell and Gene-Based Therapy for Erectile Dysfunction: Current Status and Future Needs. *Urol Clin North Am.* 2021;48:611–9.

43. Matz EL, Terlecki R, Zhang Y, Jackson J, Atala A. Stem Cell Therapy for Erectile Dysfunction. *Sex Med Rev.* 2019;7:321–8.
44. Lin CS, Xin ZC, Wang Z, Deng C, Huang YC, Lin G, et al. Stem cell therapy for erectile dysfunction: a critical review. *Stem Cells Dev.* 2012;21:343–51.
45. Salic A, Mitchison TJ. A chemical method for fast and sensitive detection of DNA synthesis in vivo. *Proc Natl Acad Sci U S A.* 2008;105:2415–20.
46. Fandel TM, Albersen M, Lin G, Qiu X, Ning H, Banie L, et al. Recruitment of intracavernously injected adipose-derived stem cells to the major pelvic ganglion improves erectile function in a rat model of cavernous nerve injury. *Eur Urol.* 2012;61:201–10.
47. Path G, Perakakis N, Mantzoros CS, Seufert J. Stem cells in the treatment of diabetes mellitus - Focus on mesenchymal stem cells. *Metabolism.* 2019;90:1–15.
48. Meier JJ, Bhushan A, Butler AE, Rizza RA, Butler PC. Sustained beta cell apoptosis in patients with long-standing type 1 diabetes: indirect evidence for islet regeneration? *Diabetologia.* 2005;48:2221–8.
49. Carlsson PO, Schwarcz E, Korsgren O, Le Blanc K. Preserved beta-cell function in type 1 diabetes by mesenchymal stromal cells. *Diabetes.* 2015;64:587–92.
50. Hu J, Yu X, Wang Z, Wang F, Wang L, Gao H, et al. Long term effects of the implantation of Wharton's jelly-derived mesenchymal stem cells from the umbilical cord for newly-onset type 1 diabetes mellitus. *Endocr J.* 2013;60:347–57.
51. Donath MY, Shoelson SE. Type 2 diabetes as an inflammatory disease. *Nat Rev Immunol.* 2011;11:98–107.
52. Chen X, Yang Q, Xie Y, Deng C, Liu G, Zhang X. Comparative study of different transplantation methods of adipose tissue-derived stem cells in the treatment of erectile dysfunction caused by cavernous nerve injury. *Andrologia.* 2021;53:e13950.
53. Ruan Y, Li M, Wang T, Yang J, Rao K, Wang S, et al. Taurine Supplementation Improves Erectile Function in Rats with Streptozotocin-induced Type 1 Diabetes via Amelioration of Penile Fibrosis and Endothelial Dysfunction. *J Sex Med.* 2016;13:778–85.
54. Liu K, Cui K, Feng H, Li R, Lin H, Chen Y, et al. JTE-013 supplementation improves erectile dysfunction in rats with streptozotocin-induced type diabetes through the inhibition of the rho-kinase pathway, fibrosis, and apoptosis. *Andrology-Us.* 2020;8:497–508.
55. Fang X, Cai Z, Wang H, Han D, Cheng Q, Zhang P, et al. Loss of Cardiac Ferritin H Facilitates Cardiomyopathy via Slc7a11-Mediated Ferroptosis. *Circ Res.* 2020;127:486–501.
56. Weiland A, Wang Y, Wu W, Lan X, Han X, Li Q, et al. Ferroptosis and Its Role in Diverse Brain Diseases. *Mol Neurobiol.* 2019;56:4880–93.
57. Belavgeni A, Meyer C, Stumpf J, Hugo C, Linkermann A. Ferroptosis and Necroptosis in the Kidney. *Cell Chem Biol.* 2020;27:448–62.

58. Stockwell BR, Friedmann AJ, Bayir H, Bush AI, Conrad M, Dixon SJ, et al. Ferroptosis: A Regulated Cell Death Nexus Linking Metabolism, Redox Biology, and Disease. *Cell*. 2017;171:273–85.
59. Li J, Cao F, Yin HL, Huang ZJ, Lin ZT, Mao N, et al. Ferroptosis: past, present and future. *Cell Death Dis*. 2020;11:88.
60. Chen S, Zhu J, Wang M, Huang Y, Qiu Z, Li J, et al. Comparison of the therapeutic effects of adiposederived and bone marrow mesenchymal stem cells on erectile dysfunction in diabetic rats. *Int J Mol Med*. 2019;44:1006–14.
61. Liu G, Sun X, Bian J, Wu R, Guan X, Ouyang B, et al. Correction of diabetic erectile dysfunction with adipose derived stem cells modified with the vascular endothelial growth factor gene in a rodent diabetic model. *PLoS ONE*. 2013;8:e72790.
62. Garcia MM, Fandel TM, Lin G, Shindel AW, Banie L, Lin CS, et al. Treatment of erectile dysfunction in the obese type 2 diabetic ZDF rat with adipose tissue-derived stem cells. *J Sex Med*. 2010;7:89–98.
63. Jeon SH, Zhu GQ, Bae WJ, Choi SW, Jeong HC, Cho HJ, et al. Engineered Mesenchymal Stem Cells Expressing Stromal Cell-derived Factor-1 Improve Erectile Dysfunction in Streptozotocin-Induced Diabetic Rats. *Int J Mol Sci*. 2018;19.
64. Kovanecz I, Vernet D, Masouminia M, Gelfand R, Loni L, Aboagye J, et al. Implanted Muscle-Derived Stem Cells Ameliorate Erectile Dysfunction in a Rat Model of Type 2 Diabetes, but Their Repair Capacity Is Impaired by Their Prior Exposure to the Diabetic Milieu. *J Sex Med*. 2016;13:786–97.

Figures

Figure 1

Primary culture and characterization of HUCMSCs. (A) Morphological features of HUCMSCs at third passage. The magnification is 100×. (B) Representative flow cytometry histograms of HUCMSCs. (C) Adipogenic differentiation of HUCMSCs assessed by Oil Red O staining. The magnification is 200×. (D) Osteogenic differentiation of HUCMSCs assessed by Alizarin Red S staining. The magnification is 200×. (E) Representative immunofluorescence results of CCSMCs show positive expression for α -SMA and desmin. The magnification is 100×. HUCMSCs: human umbilical cord mesenchymal stem cells; CCSMCs: corpus cavernosum smooth muscle cells; α -SMA: α -smooth muscle actin; DAPI: 4',6-diamidino-2-phenylindole.

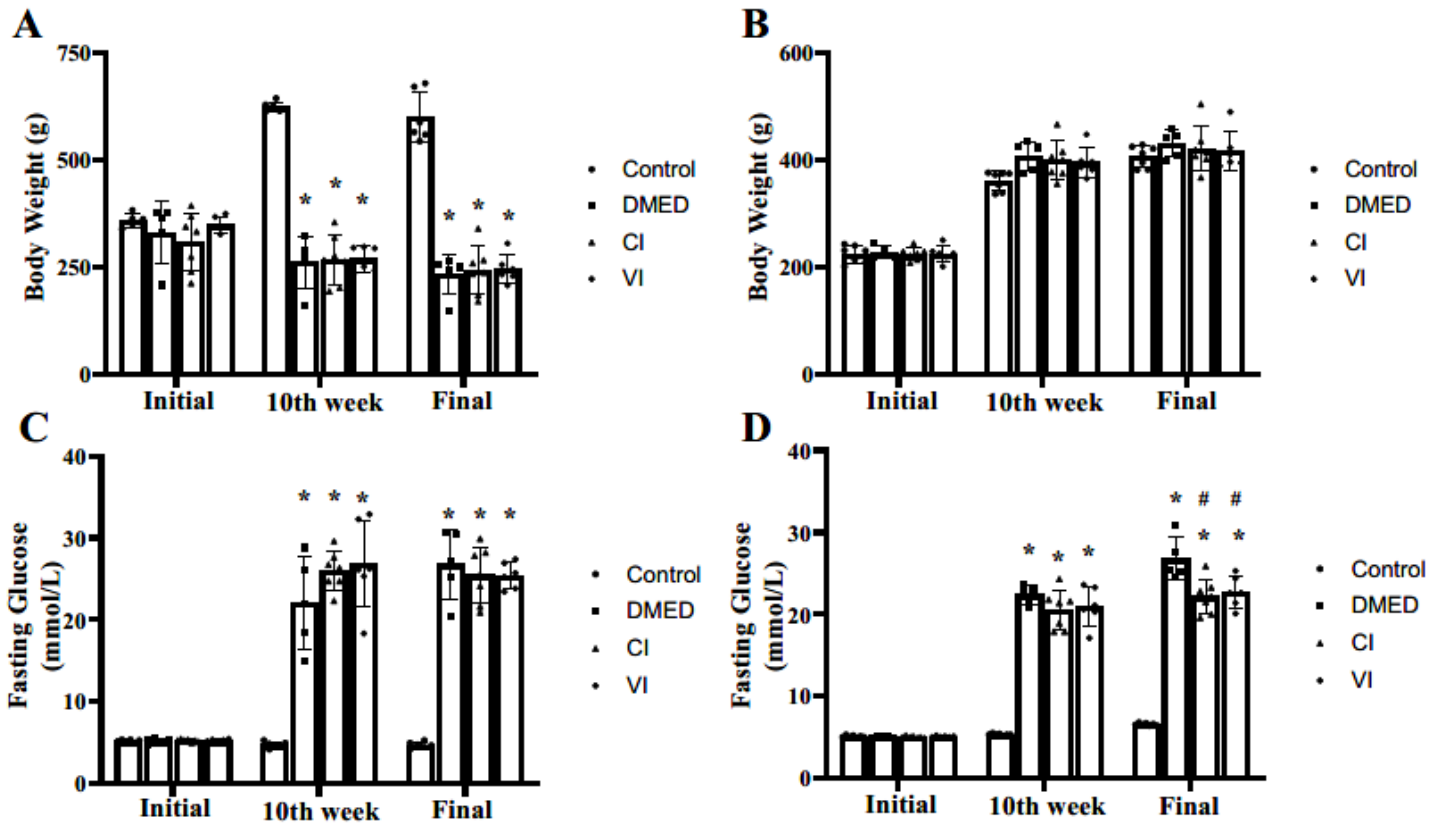


Figure 2

Metabolic status of rats. Body weights of T1DM (A) and T2DM (B) rats in each group. Fasting glucose of T1DM (C) and T2DM (D) rats in each group. Data are expressed as means \pm standard deviation. * $P < 0.05$ vs. the control group; # $P < 0.05$ vs. the DMED group. Con: control; DMED: diabetes mellitus erectile dysfunction; CI: corpus cavernosum injection; VI: tail vein injection; T1DM: type 1 diabetes mellitus; T2DM: type 2 diabetes mellitus.

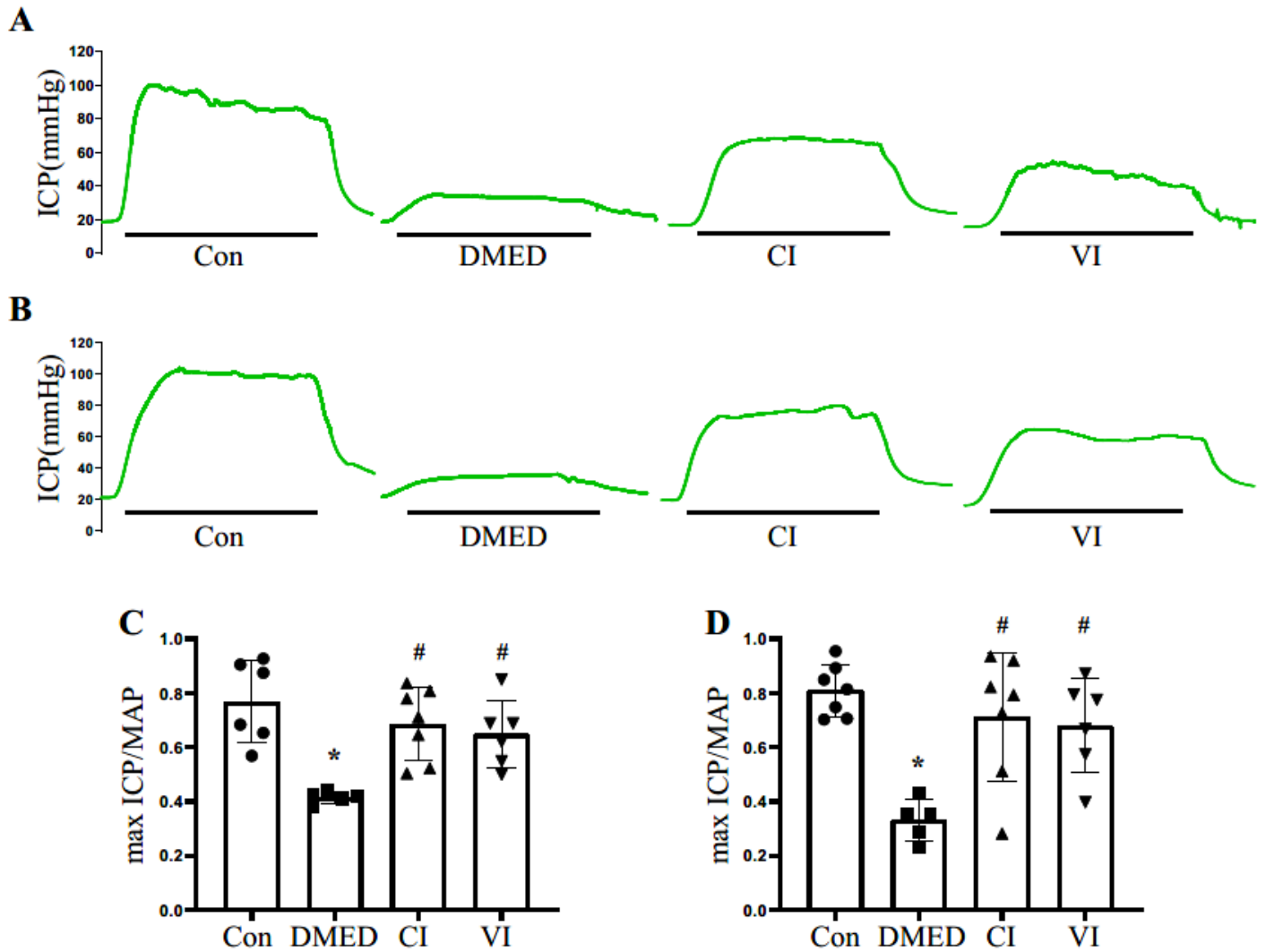


Figure 3

Evaluation of erectile function. (A) Representative ICP traces of T1DM rats (stimulation parameters: 15 Hz; 5.0 V; 1 min). (B) Representative ICP traces of T2DM rats (stimulation parameters: 15 Hz; 5.0 V; 1 min). (C) The max ICP/MAP values of each groups in T1DM rats. (D) The max ICP/MAP values of each groups in T2DM rats. Data are expressed as means \pm standard deviation. * $P < 0.05$ vs. the control group; # $P < 0.05$ vs. the DMED group. Con: control; DMED: diabetes mellitus erectile dysfunction; CI: corpus cavernosum injection; VI: tail vein injection; ICP: intracavernous pressure; MAP: mean atrial pressure.



Figure 4

Hematoxylin-eosin staining and Masson's trichrome staining of penile specimens. (A) Representative images of smooth muscle subjected to hematoxylin-eosin staining. The magnification is 100×. (B) Representative images of smooth muscle stained with Masson's trichrome staining. The magnification is 100×. (C) The ratio of smooth muscle to collagen contents in penile section of T1DM rats. (D) The ratio of smooth muscle to collagen contents in penile section of T2DM rats. Data are expressed as means \pm

standard deviation. * $P < 0.05$ vs. the control group; # $P < 0.05$ vs. the DMED group. T1DM: type 1 diabetes mellitus; T2DM: type 2 diabetes mellitus; Con: control; DMED: diabetes mellitus erectile dysfunction; CI: corpus cavernosum injection; VI: tail vein injection.

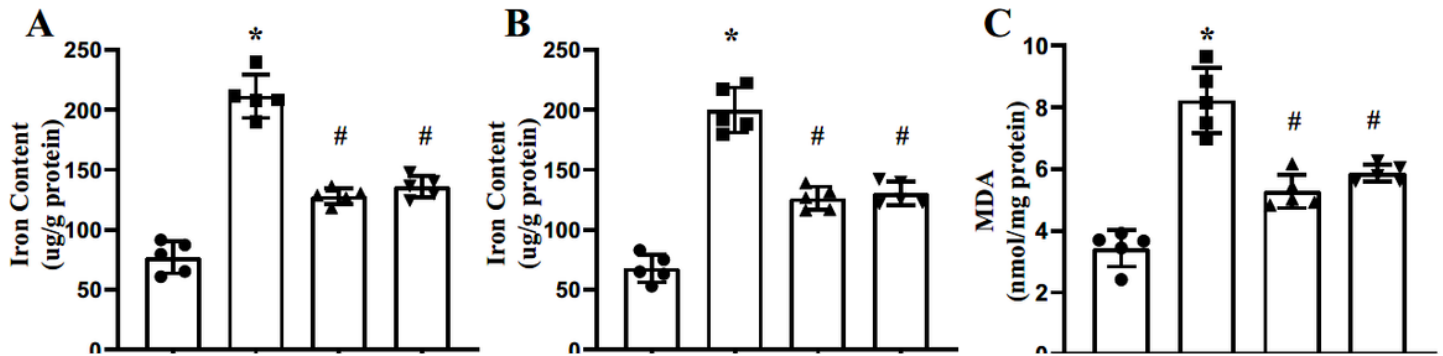


Figure 5

Assessment of iron content and oxidative activity. Iron contents in the corpus cavernosum of T1DM (A) and T2DM (B) rats. Levels of MDA in the corpus cavernosum of T1DM (C) and T2DM (D) rats. Levels of SOD in the corpus cavernosum of T1DM (E) and T2DM (F) rats. Data are expressed as means \pm standard deviation. * $P < 0.05$ vs. the control group; # $P < 0.05$ vs. the DMED group. T1DM: type 1 diabetes mellitus; T2DM: type 2 diabetes mellitus; Con: control; DMED: diabetes mellitus erectile dysfunction; CI: corpus cavernosum injection; VI: tail vein injection; MDA, malondialdehyde; SOD, superoxide dismutase.

Figure 6

Effects of HUCMSCs on reducing ROS production *in vivo*. Representative immunofluorescence ($\times 200$) (A) and quantification (B) of ROS in the corpus cavernosum of T1DM rats. Representative immunofluorescence ($\times 200$) (C) and quantification (D) of ROS in the corpus cavernosum of T2DM rats. Data are expressed as means \pm standard deviation. * $P < 0.05$ vs. the control group; # $P < 0.05$ vs. the

DMED group. ROS: reactive oxygen species; IOD: integrated option density; T1DM: type 1 diabetes mellitus; T2DM: type 2 diabetes mellitus; Con: control; DMED: diabetes mellitus erectile dysfunction; CI: corpus cavernosum injection. VI: tail vein injection; DAPI: 4',6-diamidino-2-phenylindole.

Figure 7

HUCMSCs attenuated ROS production and mitochondrial aberrations *in vitro*. (A) The diagram of the coculture system of HUCMSCs and CCSMCs. Representative immunofluorescence ($\times 200$) (B) and quantification (C) of ROS in CCSMCs of each group. (D) The morphology of the mitochondria in CCSMCs analyzed by TEM. Original magnification $\times 5.0k$ and $\times 10.0k$. Data are expressed as means \pm standard deviation. $*P < 0.05$ vs. the control group; $\#P < 0.05$ vs. the HG group. HUCMSCs: human umbilical cord mesenchymal stem cells; CCSMCs: corpus cavernosum smooth muscle cells; Con: control; HG: high glucose; Fer-1: ferrostatin-1; ROS: reactive oxygen species; IOD: integrated option density; TEM: transmission electron microscope.

Figure 8

HUCMSCs attenuated ferroptosis through the SLC7A11/GPX4/ACSL4 pathway *in vitro*. Representative immunoblot (A) and quantification (B-F) of SLC7A11, GPX4, ACSL4, LPCAT3 and ALOX15 in CCSMCs of each group. Representative immunofluorescence ($\times 200$) (G) and quantification (I) of ACSL4 in CCSMCs of each group. Representative immunofluorescence ($\times 200$) (H) and quantification (J) of GPX4 in CCSMCs of each group. Data are expressed as means \pm standard deviation. $*P < 0.05$ vs. the control group; $\#P < 0.05$ vs. the HG group. Con: control; HG: high glucose; Fer-1: ferrostatin-1; IOD: integrated option density; DAPI: 4',6-diamidino-2-phenylindole.

Supplementary Files

This is a list of supplementary files associated with this preprint. Click to download.

- [additionalfigurelegend.docx](#)
- [figureS1.pdf](#)
- [figureS2.pdf](#)